Cell Tissue Res (1990) 260:85–94

Cell and Tissue Research

Osteoclasts in teleost fish: Light- and electron-microscopical observations

Jean-Yves Sire[1], **Ann Huysseune**[2], **and François J. Meunier**[1]

[1] Equipe de Recherche 'Formations Squelettiques', UA CNRS 04 1137, Université Paris VII, Paris, France;
[2] Laboratorium voor Morfologie en Systematiek der Dieren, Gent, Belgium

Accepted January 4, 1990

Summary. This paper reports the common occurrence of osteoclasts during normal and experimental bone resorption in a number of teleost fishes. Light-microscopical observations on osteoclasts are presented in resorption areas on perichondral bone (mandibula and pharyngeal jaws of cichlids and vertebrae of gymnotids), on dermal bone (mandibula of salmonids and characoids and frontal bone of cichlids), on chondroid bone (pharyngeal jaws of cichlids), and on elasmoid body scales (cichlids and gymnotids). Osteoclasts acting along the bone surface usually lie in a Howship's lacuna whereas others are wrapped around bone extremities. Electron-microscopical observations reveal that teleost osteoclasts show features similar to those of higher vertebrate osteoclasts, e.g., the presence of a ruffled border and the occurrence of numerous vacuoles, lysosomes and mitochondria. The multinucleated aspect that characterizes osteoclasts in other vertebrate groups is not a distinct feature of teleost osteoclasts since some are possibly mononucleated. Teleost osteoclasts are also able to resorb uncalcified tissues adjoining bone resorption areas, either as a primary process directed toward the tissue (basal plate of elasmoid scale) or as a secondary phenomenon (cartilage).

Key words: Osteoclasts – Bone resorption – *Salmo fario, Myleus rhomboidalis, Eigenmannia virescens, Astatotilapia elegans, Astatotilapia burtoni, Hemichromis bimaculatus* (Teleostei)

Bone of teleost fish can be cellular (as in tetrapods) with osteocytes embedded in a mineralized matrix, or acellular, i.e., completely devoid of osteocytes (for reviews, see Moss 1963; Meunier 1987).

Send offprint requests to: Dr. Jean-Yves Sire, Laboratoire d'Anatomie comparée, Université Paris VII, 2 Place Jussieu, F-75251 Paris Cedex 05, France

Several studies on fish bone have reported resorption under various physiological conditions (Crichton 1935; Van Sommeren 1937; Tchernavin 1938a, b; Meunier and Desse 1978; Francillon et al. 1975), but the involvement of typical multinucleated osteoclasts in both cellular and acellular fish bone resorption has been the subject of a long-lasting controversy. It has often been held that bone in teleosts, under normal conditions, is resorbed without the participation of osteoclasts (Blanc 1953; Moss 1963; Ruben and Bennett 1981). Moreover, various studies dealing with experimental conditions of bone resorption have also failed to show the occurrence of multinucleated resorbing cells (Clark and Fleming 1963; Norris et al. 1963; Weiss and Watabe 1979; Wendelaar Bonga and Lammers 1982). Despite this, several papers report such osteoclasts in cellular bone both under normal and experimental conditions (Moss 1962; Lopez 1970a, b, c; Lopez and Martelly-Bagot 1971; Lopez et al. 1976; Riehl 1978; Riehl et al. 1978; Kirschbaum and Meunier 1981, 1988) in acellular bone, but only under experimental conditions (Moss 1962; Glowacki et al. 1986), in acellular 'bone' of scales (Schönbörner 1981) and in chondroid bone (Huysseune 1986). Clastic cells have also been described in resorption processes of dentin (Levi 1939; Bergot 1975; Berkovitz 1977) and in the attachment bone of teeth (Eastman 1977; Berkovitz and Shellis 1978). Most of these papers deal with classical histological techniques. As far as we know, only one electron-microscopical study (Glowacki et al. 1986) shows typical ultrastructural features of multinucleated osteoclasts after experimental induction of bone resorption.

This paper reports osteoclastic bone resorption in normal and experimental conditions in a variety of teleost fishes possessing either cellular or acellular bone, thereby stressing its importance in bone destruction and remodeling processes. This study also presents a number of electron-microscopical observations on multinucleated and possibly mononucleated teleost osteoclasts.

Materials and methods

Morphological data were collected from 3 cellular-boned teleost species: a salmoniform (*Salmo fario*), a characiform (*Myleus rhomboidalis*), and a gymnotiform (*Eigenmannia virescens*), and from 3 acellular-boned perciforms (the mouth-brooding cichlid species *Astatotilapia elegans*, its close relative *A. burtoni*, and the substrate-brooding cichlid species *Hemichromis bimaculatus*, all bred in the laboratory) (classification after Nelson 1984).

Light microscopy

Paraffin. Adult specimens of *M. rhomboidalis* and *S. fario* were fixed in Bouin's and routinely processed for paraffin embedding and sectioning. Sections were stained using Gabe's trichrome for *M. rhomboidalis* or red solid/picro-indigo-carmine for *S. fario*.

Epon. Specimens of various developmental stages of *A. elegans*, *A. burtoni* and *H. bimaculatus*, adult body scales of *H. bimaculatus* and regenerating tails (8 days) of *E. virescens* (for details, see Kirschbaum and Meunier 1981) were fixed for transmission electron-microscopical observations (see below). Experimentally grafted (*H. bimaculatus*) and resorbing (*E. virescens*) scales were also used.

Serial semithin sections (1 or 2 μm thick) were cut from selected head regions, tail and scales, and were stained using toluidine blue.

Transmission electron microscopy (TEM)

Specimens of *A. burtoni*, *H. bimaculatus*, isolated scales of *H. bimaculatus*, and regenerating tails of *E. virescens* were fixed as described previously (Sire 1985). Briefly, samples were immersed for 2 h in a mixture of 1.5% glutaraldehyde and 1.5% paraformaldehyde in 0.1 M cacodylate buffer, rinsed in buffer with 10% sucrose, postfixed for 2 h in 1% OsO_4 in 0.1 M cacodylate buffer with 8% sucrose, rinsed, dehydrated and embedded in Epon. Except for the tails of *E. virescens*, samples were decalcified for 5–7 days with 0.1 M EDTA added to the fixative mixture. Specimens of *A. elegans* were fixed according to the method of Hirsch and Fedorko (1968) and subsequently embedded in Epon.

Thin sections were obtained using a Reichert OMU2 ultratome equipped with a diamond knife. They were contrasted with uranyl acetate and lead citrate, and observed in a Philips EM 201 transmission electron microscope operating at 80 kV.

Results

Light-microscopical observations

Lower jaw. Osteoclasts have been frequently encountered in the mandibula, both during early ontogeny and during later remodeling of the lower jaw (Figs. 1–4).

In larval *Astatotilapia burtoni*, small flattened osteoclasts (10 μm long, 7 μm wide and mono- or at most bi-nucleated) are found wrapped around the extremity of the remains of the perichondral bone surronding Meckel's cartilage (Fig. 1). In such cases, the cells do not lie in a Howship's lacuna. Isolated small flattened osteoclasts (15–20 μm long, at most 10 μm wide and most probably mononucleated) attacking perichondral bone in a similar situation are found in *Hemichromis bimaculatus* (Fig. 2). Moreover, in both species, the osteoclasts resorbing perichondral bone apparently act simultaneously on the adjacent cartilage matrix (Figs. 1, 2).

During later development, large (40–70 μm long, 40 μm high) globular multinucleated (7–15 nuclei in the section) osteoclasts are found along the dentary (dermal

Figs. 1–10. Light micrographs showing various examples of osteoclastic bone resorption in different teleost species with acellular (Figs. 1, 2, 5–7, 10) or cellular bone (Figs. 3, 4, 8, 9). Figs. 1, 2, 5–10: Epon-embedded samples, toluidine blue staining; Figs. 3, 4: paraffin-embedded samples

Fig. 1. *Astatotilapia burtoni.* Larval specimen (6.5 mm in standard length (SL)). Resorption of Meckel's cartilage (*mc*) and perichondral bone (*p*) in the region adjacent to a tooth germ (*t*). The *arrow* points toward an osteoclast (for details, see Figs. 18, 20). *Bar:* 25 μm; ×600

Fig. 2. *Hemichromis bimaculatus.* Larval specimen (5 mm SL). Resorption of Meckel's cartilage (*mc*) and perichondral bone (*p*) in the region adjacent to a tooth germ (*t*). The *arrow* points toward an osteoclast (for details, see Fig. 11). *Bar:* 25 μm; ×600

Fig. 3. *Salmo fario.* Adult specimen. Resorption of the dentary (*d*) in the area facing a developing tooth (*t*). Multinucleated osteoclasts (*arrows*) are seen in Howship's lacunae. Solid red/picro-indigo-carmine. *Bar:* 100 μm; ×150

Fig. 4. *Myleus rhomboidalis.* Adult specimen. Resorption of dentary (*d*) by multinucleated osteoclasts (*arrows*). Gabe's trichrome. *Bar:* 50 μm; ×250

Fig. 5. *Astatotilapia elegans.* Juvenile specimen (7.5 mm SL). Resorption of perichondral bone (*p*) in the pharyngeal jaws. The *arrow* points toward an osteoclast (for details, see Fig. 12). *Bar:* 10 μm; ×900

Fig. 6. *Hemichromis bimaculatus.* Juvenile specimen (8 mm SL). Resorption of chondroid bone (*cb*) in the pharyngeal jaws. The *arrow* points toward an osteoclast (for details, see Fig. 14). *Bar:* 25 μm; ×600

Fig. 7. *Hemichromis bimaculatus.* Juvenile specimen (10 mm SL). Transverse section of the part of the frontal bone (*f*) surrounding the supraorbital canal (*sc*). The *arrows* point toward an osteoclast (for details, see Fig. 13); *b* brain; *tm* taenia marginalis. *Bar:* 50 μm; ×250

Fig. 8. *Eigenmannia virescens.* Transverse section of a wounded vertebra, 8 days after amputation of the caudal peduncle of an adult specimen. Note the 2 large multinucleated osteoclasts (*arrows*) lining the bone surface (for details, see Fig. 15). *Bar:* 50 μm; ×250

Fig. 9. *Eigenmannia virescens.* Transverse section of a scale in the wounded region near the amputated caudal peduncle. Five multinucleated osteoclasts are seen along both sides of the scale (for details, see Fig. 16). The scale has been artifactually split during sectioning; *bp* basal plate; *el* external layer. *Bar:* 10 μm; ×800

Fig. 10. *Hemichromis bimaculatus.* Adult specimen. Longitudinal section of a body-scale 15 days after autotransplantation with reversal of polarity (upside down); posterior region of the scale. A multinucleated osteoclast is seen along a large part of the scale (for details, see Figs. 17, 21, 22); *bp* basal plate; *el* external layer. *Bar:* 10 μm; ×700

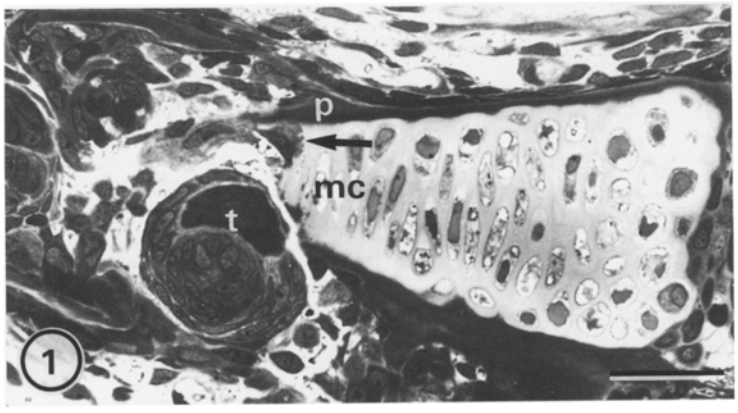
p
mc
t
1

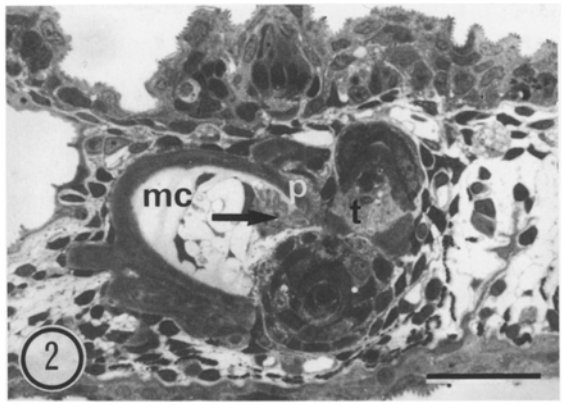
mc
p
t
2

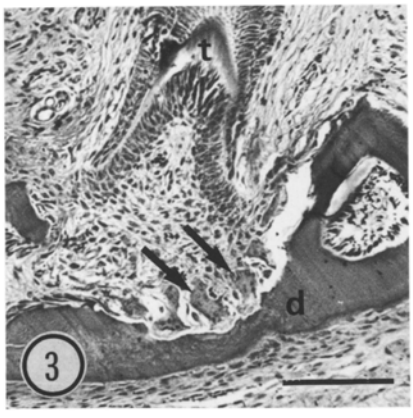
t
d
3

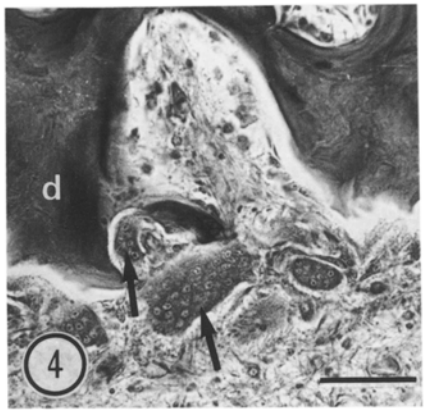
d
4

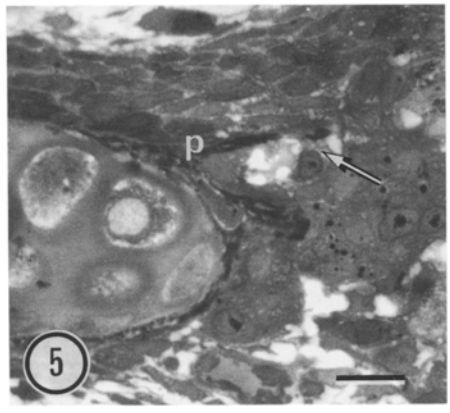
p
5

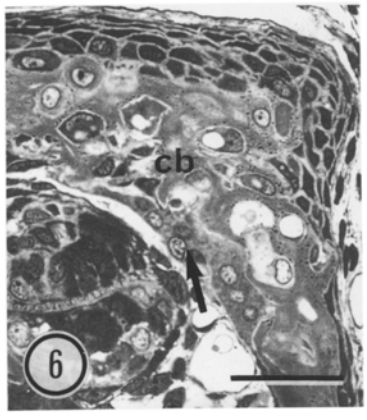
cb
6

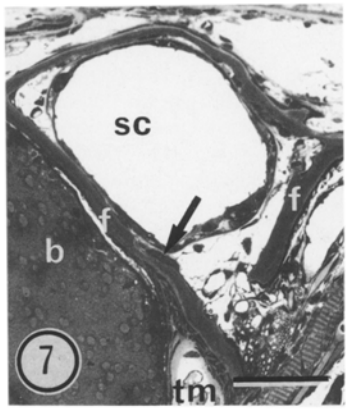
sc
f
f
b
7
tm

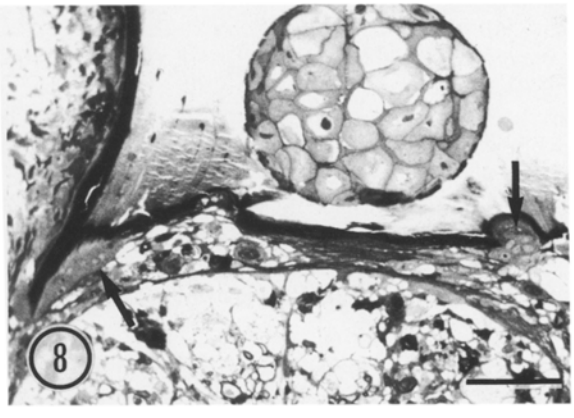
8

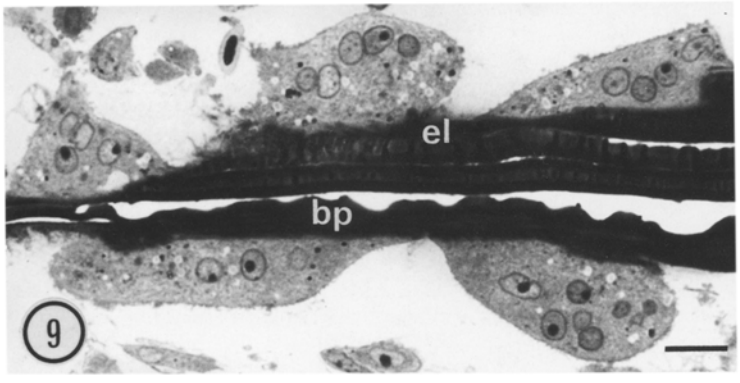
el
bp
9

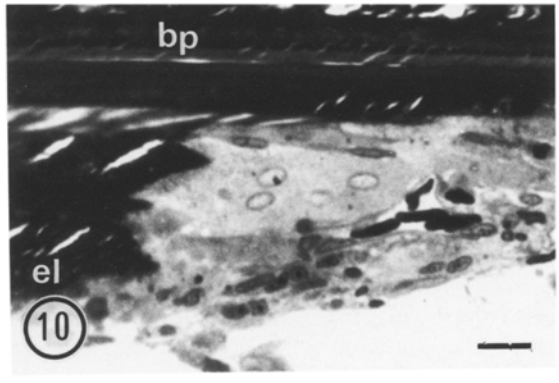
bp
el
10

bone) in fishes of 2 super-orders, the cellular-boned protacanthopterygian *Salmo fario* (Fig. 3) and the cellular-boned ostariophysan *Myleus rhomboidalis* (Fig. 4). The osteoclasts are apposed to the bone surface and usually lie in a typical Howship's lacuna.

Pharyngeal jaw. In larval *Astatotilapia elegans,* isolated resorbing cells can be found wrapped around the edges of the remains of the perichondral bone or its apolamellae that surround the cartilage of the upper pharyngeal jaws. As on the lower jaw, these osteoclasts do not lie in a typical Howship's lacuna (Fig. 5).

Chondroid bone, which develops on the upper pharyngeal jaws in a later stage (see Huysseune 1986 and Huysseune and Verraes 1986), is subjected to erosion along its proximal (ventral) side to accommodate teeth of new generations developing from below. Multinucleated cells are responsible for this resorption and have been observed in *A. elegans,* both in young chondroid bone (fishes of 1 month of age) and mature chondroid bone (fishes of several months old) (cf. light micrographs published by Huysseune 1986). Osteoclasts attacking chondroid bone in the same position in young *Hemichromis bimaculatus* are shown in Fig. 6.

Frontal bones. The neurodermal component of the frontal bones in *H. bimaculatus* (the part surrounding the supraorbital canal) presents a scalloped surface created by Howship's lacunae that are occupied by isolated flattened cells involved in bone matrix removal (Fig. 7). Numerous observations of 1 μm-thick serial sections have not been able to establish whether these cells are mono- or multinucleated. If some are multinucleated, they certainly contain no more than two or three nuclei. These resorbing cells are 20–25 μm long, 30–40 μm wide, and 8–10 μm high.

All instances reported so far concern the normal development of the skeletal elements involved. Two further examples concern osteoclastic bone resorption during conditions of experimental bone destruction or regeneration.

Vertebrae. Eigenmannia virescens regenerates a bony rod after amputation of a large part of its caudal peduncle (Meunier and Kirschbaum 1978; Kirschbaum and Meunier 1981). During the first few days following amputation, the wounded vertebra is subjected to resorption. Numerous large (30–70 μm long, 20 μm high) globular multinucleated (5–7 nuclei in the section) osteoclasts lie in Howship's lacunae against the inner surface of the vertebral bone (Fig. 8).

Scales. The scales of *Eigenmannia virescens* and *Hemichromis bimaculatus* belong to the elasmoid type, i.e., they are thin lamellar collagenous plates composed of a basal plate (isopedin), covered by a thin superficial layer with its outer limiting layer. After amputation of the caudal peduncle of *Eigenmannia virescens,* osteoclastic resorption involves the scales located in the wounded region. Numerous large (40–60 μm long, 15–20 μm high) globular multinucleated (3–8 nuclei in the section) osteoclasts are located on both sides of the scales (Fig. 9). They are therefore involved in the erosion of both the well-mineralized superficial layer and the unmineralized lower part of the isopedin. Twenty or more osteoclasts can be observed simultaneously on one section. Autotransplantation of scales with reversal of their polarity (upside down) in *Hemichromis bimaculatus* induces partial resorption of the posterior region of the scale. Large (50 μm long, 20 μm high) globular multinucleated osteoclasts, located in Howship's lacunae, attack this part of the scale, generally along its insertion into the scale pocket (Fig. 10). They are simultaneously involved in the resorption of both the well-mineralized superficial layer (outer limiting layer) and the unmineralized lower part of the isopedin.

Electron-microscopical observations

Figs. 11–22 present different shapes of osteoclasts involved in the resorption of various bone matrices, such as perichondral bone (Figs. 11, 12, 15, 18–20), dermal

Figs. 11–22. TEM micrographs showing details of osteoclasts involved in the resorption of different types of bone in various teleost species. Some of these micrographs are details of general views of sections (or adjacent sections) presented as light micrographs (Figs. 1–10)

Fig. 11. *Hemichromis bimaculatus* (5 mm SL). See Fig. 2. Osteoclast wrapped around the extremity of perichondral bone (*p*) surrounding Meckel's cartilage (*mc*). Note the nearby presence of a tooth germ (*t*). The osteoclast possesses a well-developed ruffled border (*RB*), large vacuoles (*V*), 2 clear zones (*C*) of attachment and numerous mitochondria (*M*) and free ribosomes. A single nucleus (*N*) is visible in the section. Note the few extensions of the osteoclast membrane penetrating the cartilage matrix (*arrow*). *Bar:* 2 μm; ×6800

Fig. 12. *Astatotilapia elegans* (7.5 mm SL). See Fig. 5. Osteoclastic resorption of a fragment of perichondral bone (*p*) remaining after complete resorption of the pharyngobranchial cartilage. The osteoclast completely wraps the extremity of the bone fragment. Close to the osteoclast membrane, the collagen fibrils are disassembled, sectioned and dissolved. Note the presence of patches of electron-dense particles (*arrows*) within large vacuoles (*V*). *C* clear zones of attachment; *RB* ruffled border. *Bar:* 1 μm; ×15000

Fig. 13. *Hemichromis bimaculatus* (10 mm SL). See Fig. 7. Flattened osteoclast attacking the frontal bone matrix (*f*) in a region close to the supraorbital canal. Note the well-developed ruffled border, numerous vacuoles, and mitochondria. The osteoclast is located in a narrow space between the epithelium (*e*) lining the supraorbital canal and the frontal bone. On the opposite side of the bone, facing the osteoclast, several active osteoblasts (*ob*) are seen. *Bar:* 3 μm; ×4500

Fig. 14. *Hemichromis bimaculatus* (8 mm SL). See Fig. 6. Osteoclastic resorption of chondroid bone matrix (*cb*). The ruffled border (*RB*) is less developed compared with that of osteoclasts shown in the previous micrographs. Vacuoles of various sizes, mitochondria, free ribosomes and Golgi zones are numerous. Two nuclei (*N*) are visible in the osteoclast. In the upper part of the micrograph, the osteoclast is in contact with a chondroid bone cell (*cc*) after resorption of the matrix surrounding this cell and the opening of the lacuna in which it is located. *Bar:* 2 μm; ×8000

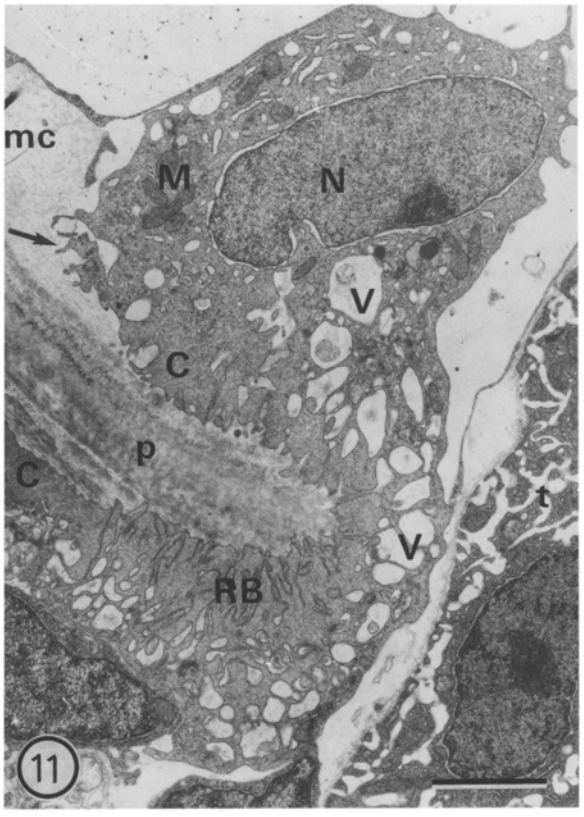
mc
M
N
V
C
p
C
t
V
RB
11

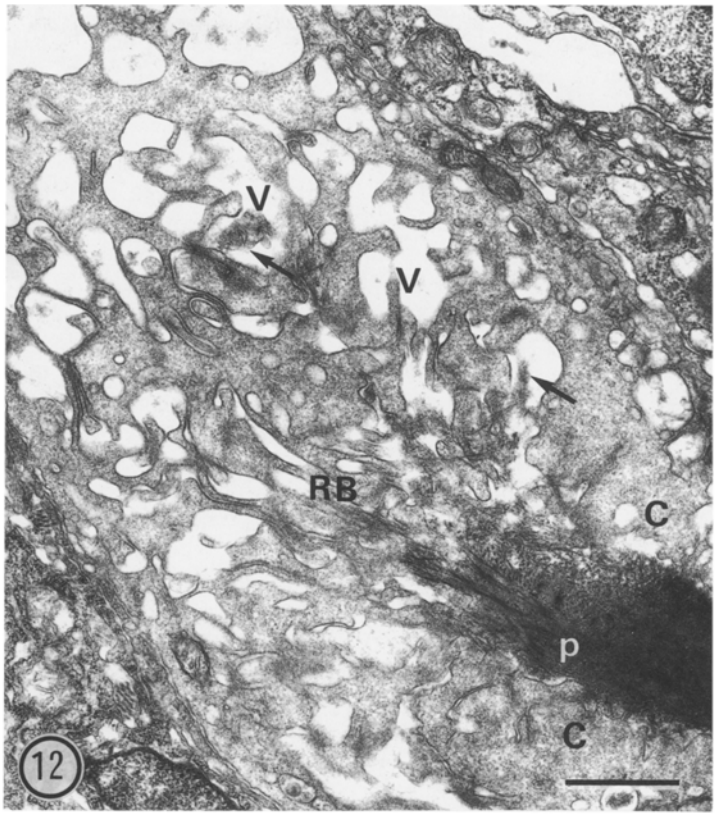
V
V
RB
C
p
C
12


f
oc
ob
e
13

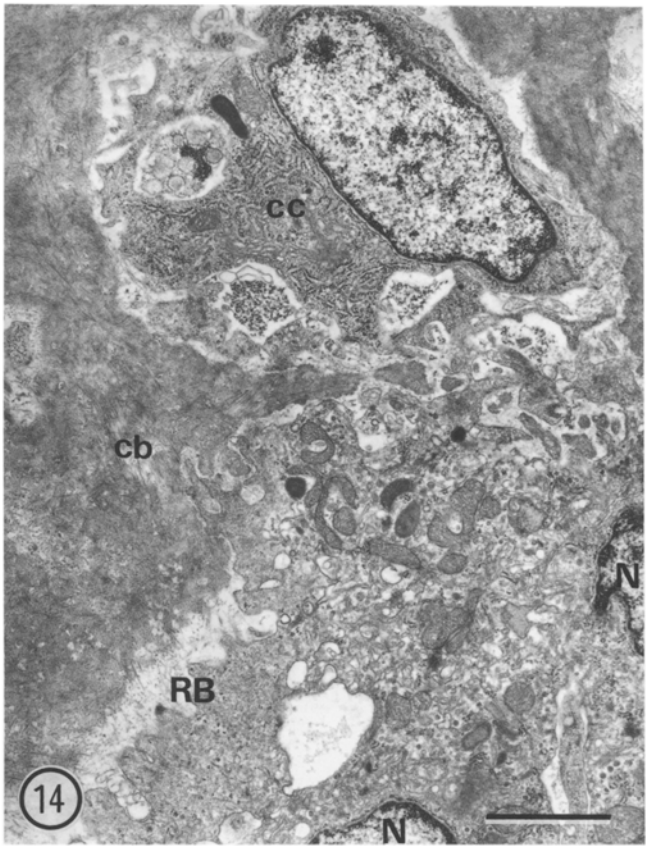
cc
cb
N
RB
N
14

bone (Fig. 13), chondroid bone (Fig. 14), and scales (Figs. 16, 17, 21, 22). In all these cases, osteoclasts are characterized by an extensive ruffled border, lysosomes, numerous mitochondria, free ribosomes, extensive Golgi zones, and numerous large vacuoles located near the resorption area. Some of them contain electron-dense material. In small flattened cells, only one nucleus is visible, or is absent in the section (Figs. 11–13, 19), whereas in large, generally globular osteoclasts several nuclei may be seen (Figs. 14, 16). The ultrastructural features (ruffled border, vacuoles) of osteoclasts attacking comparable matrices, resemble each other, e.g., in perichondral (Figs. 11, 12) or in dermal bones (Fig. 13), both of which are composed of parallel-fibered bone. The ruffled border may have a different aspect in osteoclasts resorbing chondroid bone (woven-fibered bone, Fig. 14), scales (lamellar bone and collagen-poor matrix, Figs. 16, 17) or cartilage (uncalcified loose collagenous stroma, Figs. 11, 18). In chondroid bone, the osteoclast border may be apposed to a chondroid cell, the lacuna of which has been opened during the process of resorption (Fig. 14). The aspect of the ruffled border is especially striking in the case of cichlid scale resorption (Fig. 17). Depending on the orientation of the collagen fibrils in the isopedin (plywood-like structure), the osteoclast produces at least 2 types of cell extensions. When the collagen fibrils are oriented perpendicular to the surface of the attacking osteoclast, extremely long cell extensions penetrate deeply into the scale, among the fibrils (Fig. 22); similar cell extensions are observed when the osteoclast resorbs a matrix poor in collagen fibrils, e.g., the outer limiting layer of the scale (Fig. 17) or a cartilaginous stroma (Figs. 11, 18). In contrast, when the collagen fibrils are oriented parallel to the attacking osteoclast surface, the latter forms an elaborate, but compact, ruffled border (Fig. 21). In all the studied osteoclasts, vacuoles that contain small patches of electron-dense granular or fibrillar material are located below the ruffled border. In some cases, the effect of osteoclastic resorption on the collagenous matrix is clearly visible. Indeed, when sectioned transversely, it is clear that the collagen fibrils decrease in diameter toward the cell membrane and appear to be progressively dissolved (Fig. 21). When the collagen fibrils are sectioned longitudinally, each fibril seems to be first disassembled, then sectioned before being dissolved (Figs. 12, 21, 22). In areas of perichondral bone resorption (mandibula, pharyngeal jaws), it has often been observed that a small part of the osteoclast border extends small processes into the adjacent cartilage matrix (Figs. 11, 18).

Discussion

Osteoclasts in osteichthyan bones

The present work demonstrates that osteoclasts are involved in the process of bone resorption (in acellular and cellular bone species), under both normal and experimental conditions. Osteoclasts are present in different species of teleosts phylogenetically as distant (Nelson 1984) as *Salmo fario* (Protacanthopterygii), *Myleus rhomboidalis* and *Eigenmannia virescens* (Ostariophysi), and cichlids (Acanthopterygii). This confirms and extends other data, reporting osteoclasts in teleost fishes. Moreover, the presence of Howship's lacunae (as evidence of osteoclastic activity) has been reported in other osteichthyans, such as the salmonid *Salmo salar* (Meunier and Desse 1978), the cyprinodontid *Orestias albus* and the acanthurid *Acanthurus dussumieri* (Meunier 1983), and the dipnoans (Géraudie and Meunier 1984). We conclude that osteoclasts are common bone-resorbing cells in osteichthyan fish under both normal and experimental conditions.

This study shows that osteoclasts resorb dermal, perichondral, and endochondral bones. This extends the observations reported in the literature mainly on dermal and endochondral bone. Therefore, osteoclastic bone resorption in teleosts seems to be independent of the developmental origin of the matrix.

Osteoclasts resorb bone of different structural types (cellular, acellular and chondroid bone). Until now, osteoclastic bone resorption under normal conditions has only been reported in species with cellular bone (Lopez 1970a, b, c; Moss 1962; Riehl 1978; Riehl et al. 1978)

Fig. 15. *Eigenmannia virescens.* Adult specimen. See Fig. 8. Osteoclastic resorption of the vertebral bone (*v*) 8 days after amputation of the caudal peduncle. Detail of the ruffled border (*RB*). *Bar:* 3 μm; ×4500

Fig. 16. *Eigenmannia virescens.* Same section as in Fig. 15. See Fig. 9. A large multinucleated osteoclast is seen along the uncalcified basal plate of a scale (*s*). Note the penetration of the ruffled border into the collagenous matrix. *Bar:* 1 μm; ×10500

Fig. 17. *Hemichromis bimaculatus.* Adult specimen. See Fig. 10. Fifteen days after transplantation upside down, the scale is found lying by an osteoclast for a considerable part of its thickness. The ruffled border (*RB*) is extremely well developed in the region where it is resorbing the plywood-like structure of the collagenous fibrils of the basal plate of a scale (*s*). Note the presence of a few extensions (*arrow*) penetrating the outer limiting layer of the scale. There is no nucleus visible in this region; numerous mitochondria can be seen. *Bar:* 5 μm; ×2300

Fig. 18. *Astatotilapia burtoni* (6.5 mm SL). See Fig. 1. The osteoclast located along the mandibular perichondral bone (*p*) does not show a typical ruffled border as in the osteoclast of Fig. 11. Nevertheless, the osteoclast border adjoining the cartilage matrix (*mc*) shows digitations (*arrow*), a dense cytoplasmic border and numerous vacuoles. Note that the tooth germ (*t*) is very close to the osteoclast. *Bar:* 1 μm; ×11300

Fig. 19. *Astatotilapia burtoni* (7.3 mm SL). Osteoclastic resorption of the perichondral bone (*p*) surrounding Meckel's cartilage (*mc*). Part of an osteoclast has penetrated the cartilage and is resorbing the bone from the inside. *Bar:* 2 μm; ×6800

Fig. 20. *Astatotilapia burtoni.* Detail of an osteoclast border close to the mandibular perichondral bone (same specimen as in Figs. 1 and 18). Digitations with electron-dense cytoplasm penetrate the cartilage matrix. *Bar:* 500 nm; ×30000

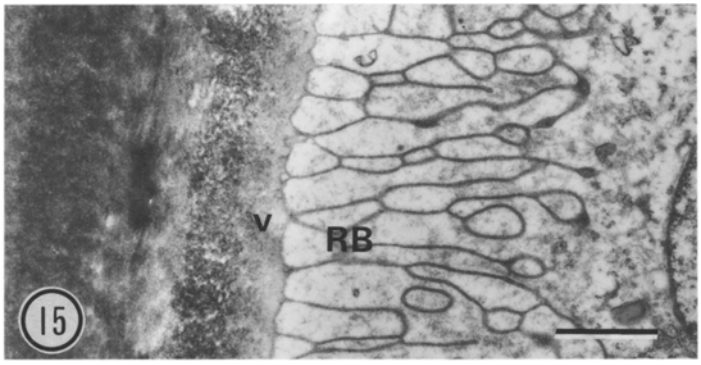
v
RB
15

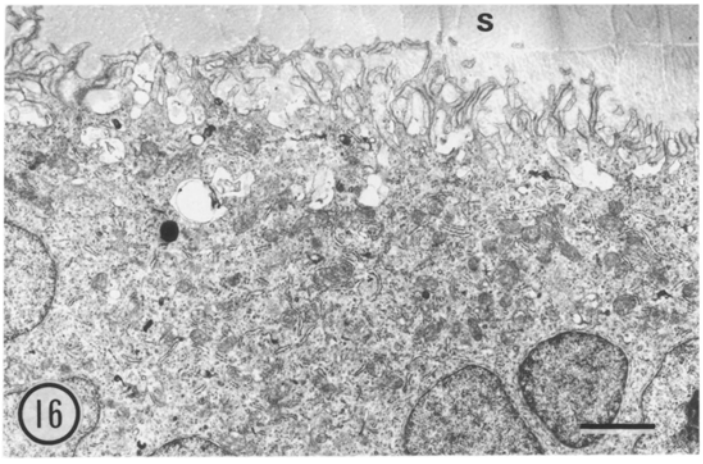
s
16

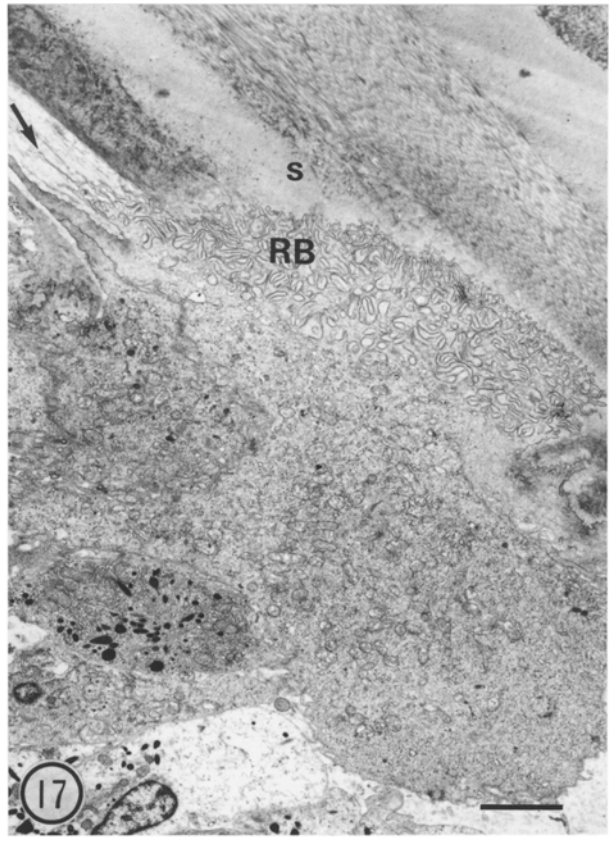
s
RB
17

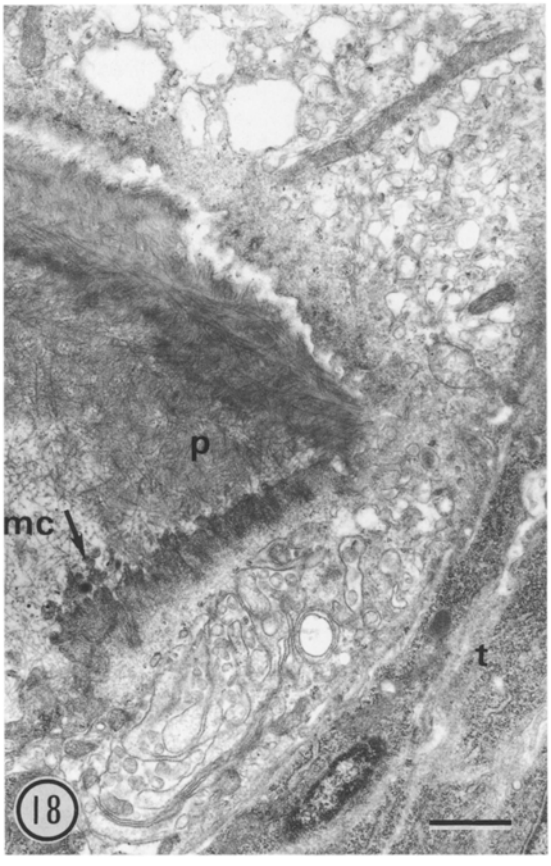
p
mc
t
18

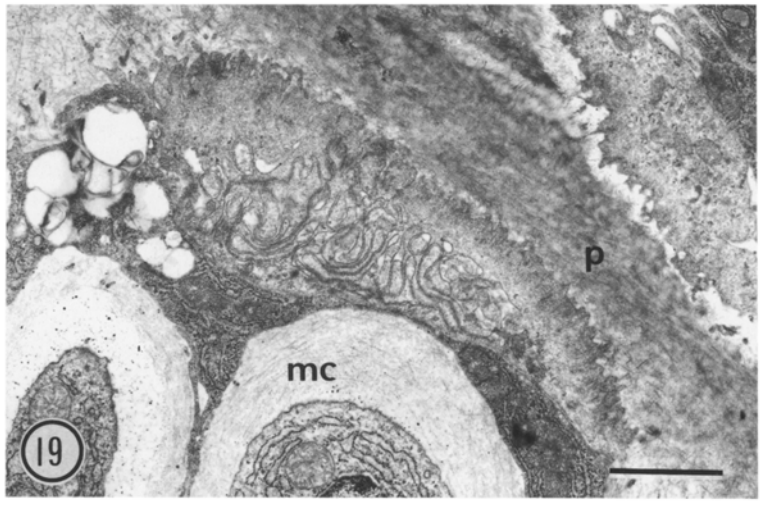
p
mc
19

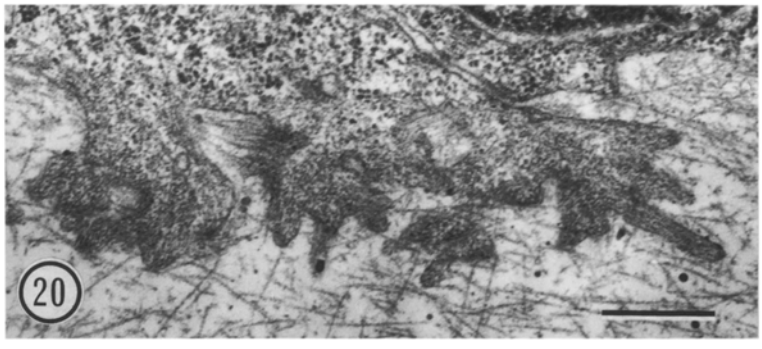
20

Fig. 21. *Hemichromis bimaculatus.* Detail of the border of the osteoclast of Fig. 17. The transversely sectioned collagen fibrils of the scale (*s*) show a decrease in diameter close to the osteoclast membrane (*arrow*). *Bar:* 500 nm; ×30000

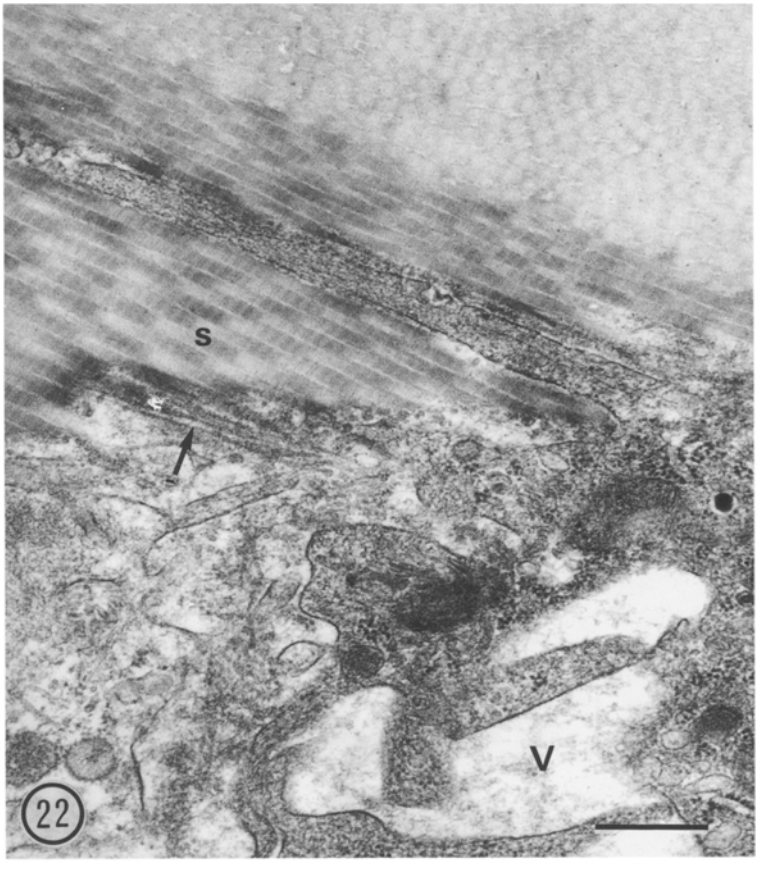

Fig. 22. *Hemichromis bimaculatus.* Same specimen as in Figs. 10 and 17. Detail of the osteoclast border along the basal plate of the scale (*s*). A cytoplasmic process penetrates deeply into the collagenous layer in which the fibrils are oriented longitudinally. The edge of the layer in direct contact with the osteoclast shows the dissociation of the collagen fibrils into microfibrils (*arrow*). *V* vacuole. *Bar:* 500 nm; ×30000

and therefore has long been considered a particular feature of this type of bone. Although several studies have failed to show osteoclasts in normal acellular bone (Moss 1961; Clark and Fleming 1963; Norris et al. 1963; Ekanayake and Hall 1987, 1988), osteoclasts have been found in acellular bone after experimental procedures (Schönbörner 1981; Glowacki et al. 1986). Our results show that typical osteoclasts can be commonly observed under normal conditions in acellular bone (mandibula, pharyngeal jaws, frontal bone of cichlids), leading to the assumption that the presence of osteocytes is not a prerequisite for the existence of osteoclasts. The origin of teleost osteoclasts remains unknown, but it is now well established that osteoclasts in higher vertebrates do not arise from osteocytes but from progenitor cells originating in hematopoietic tissues (for recent reviews, see Marks and Popoff 1988; Vaes 1988).

In contrast to the large, generally globular, numerous and easily recognizable osteoclasts involved in experimental resorption, the small flattened isolated osteoclasts described here are difficult to distinguish using light microscopy; indeed, they have only been identified as such by their ultrastructural characteristics. This may explain why they have been largely overlooked in the past.

Ultrastructure of fish osteoclasts

The ultrastructural features of fish osteoclasts are similar to those of mammalian osteoclasts (cf. Dhem 1971; Hancox 1972; Jones and Boyde 1977; and recent reviews by Marks and Popoff 1988; Vaes 1988). The differences between fish and mammalian osteoclasts are mainly related to size and shape.

The shape of osteoclasts is not strictly related to the localization on the bone surface, e.g., small flattened osteoclasts may be found either wrapped around a bone extremity (perichondral bone of the lower jaw of larval cichlids) or lying in a shallow lacuna along the bone surface (frontal bone of juvenile cichlids). Large globular osteoclasts are found in deep typical Howship's lacunae (dentary of adult salmonids and characoids, cichlid scales) or along the bone surface (gymnotoid scales).

Small flattened osteoclasts are commonly observed in areas in which there is limited space available for the cell to attack the bone surface, e.g., between a tooth germ and the bone (mandibula and pharyngeal jaws of larval cichlids) or between the supraorbital canal and the bone (frontal bone of juvenile cichlids). In contrast, globular-shaped osteoclasts are commonly encountered in regions where there is no limitation of space, e.g., around vertebrae and scales, or in the large lacunae in bone implants (Glowacki et al. 1986).

The flattened shape of osteoclasts makes it difficult to determine whether such resorbing cells are multinucleated; observations on serial sections lead to the assumption that some of these active osteoclasts may be mononucleated. On the other hand, the globular type of osteoclasts always shows several nuclei. Some authors have considered the possibility that mononucleated cells in teleost fish are responsible for bone matrix resorption (Weiss and Watabe 1979; Bordat 1987), but the cells presented in their work do not possess the typical features of the possibly mononucleated osteoclasts that we have described (ruffled border, numerous vesicles, clear zones of attachment, vacuoles). The resorbing mononucleated cells reported by the former authors could be closely related to macrophages. On the other hand, the role of mammalian monocytes and macrophages in the resorption of living bone is still a matter of controversy (cf. Mundy et al. 1977; Kahn et al. 1978; Chambers and Horton 1984). We think that the mononucleated osteoclasts in fish could be closer to functional preosteoclasts described in mammals than to macrophages. If so, the fusion of preosteoclasts into multinucleated osteoclasts would not be a necessary condition for yielding functional bone-resorbing cells in fish.

It appears that the organization of the ruffled border may change according to the structure of the organic matrix that the osteoclast is attacking. The ruffled border is very elaborate when the matrix is dense and probably difficult to penetrate (parallel-fibered or lamellar collagenous matrix: perichondral and dermal bone, and scales, respectively) whereas it is much less elaborate and shows only a few extensions when the matrix is loose (cartilage, upper layer of the scale). Although mammalian osteoclasts preferentially resorb mineralized matrices, they appear to be able to attack adjacent uncalcified matrices as well (cf. Vaes 1988). This also seems to be the case here (cf. resorption of cartilage and the deep part of the isopedin). In the case of the experimental resorption of the scales of *Eigenmannia virescens*, typical multinucleated osteoclasts directly attack the uncalcified surface of the isopedin, without contact with the mineralized part of the scale. Thus, in this particular case, osteoclast-like cells attack uncalcified matrix, although it is commonly considered that the presence of a mineral phase is a prerequisite for osteoclastic activity in mammals (see Vaes 1988). However, we should note that the uncalcified isopedin of fish scales is considered to be a bone-derived tissue (Meunier 1987). Another 'activating substance' (instead of mineral) may be present in isopedin and, perhaps, in normal bone.

The examples of physiological osteoclastic resorption presented in this paper are always associated with areas of intense remodeling, such as those found in dentigerous areas (oral and pharyngeal jaws) and in the reshaping of bones (frontal bone). Thus, it appears that fish osteoclasts play a similar role to mammalian osteoclasts (e.g., bone modeling and remodeling).

Experimental resorption after grafting of the scales of *Hemichromis bimaculatus* with reversal of the scale polarity can be related to a reshaping of the posterior region of the scale to regain its original convex shape. Resorption of the caudal skeleton of *Eigenmannia virescens* cleans the bone surfaces before regeneration of the tail (Kirschbaum and Meunier 1981, 1988). Interestingly, these experimental conditions involve numerous large osteoclasts and can therefore be considered suitable models for further investigations on osteoclast recruitment and osteoclast physiology in teleost fish.

Acknowledgements. The authors are very grateful to Dr. J.P. Denizot (Département de Neurophysiologie, CNRS, Gif-sur-Yvette, France) for providing fixed regenerating tails of *Eigenmannia virescens*, and to Drs. H. Francillon and F. Lecomte (Laboratoire d'Anatomie comparée, Université Paris 7, France) for providing sections of the mandibulae of *Salmo fario* and *Myleus rhomboidalis*, respectively. We thank Dr. M. Whitear (Department of Biology, University College London) and Dr. G. Vaes (Université Catholique de Louvain, Laboratoire de Chimie physiologique, Belgique) for their comments on the manuscript. F. Allizard and G. De Wever are acknowledged for their expert technical assistance in block sectioning. The second author acknowledges a grant of the FKFO 2.9005.84. This work was performed within the framework of an International Program of Cooperation between France (CNRS/DRCI) and Belgium (Ministry of the Flemish Community).

References

Bergot C (1975) Morphogenèse et structure des dents d'un téléostéen (*Salmo fario* L.). J Biol Buccale 3:301–324

Berkovitz BKB (1977) Chronology of tooth development in the rainbow trout (*Salmo gairdneri*). J Exp Zool 200:65–70

Berkovitz BKB, Shellis RP (1978) A longitudinal study of tooth succession in piranhas (Pisces: Characidae), with an analysis of the tooth replacement cycle. J Zool (Lond) 184:545–561

Blanc M (1953) Contribution à l'étude de l'ostéogenèse chez les Poissons Téléostéens. Mém Mus Hist Nat (Paris) VII:1–145

Bordat C (1987) Etude ultrastructurale de l'os des vertèbres du Sélacien *Scyliorhinus canicula* L. Can J Zool 65:1435–1444

Chambers TJ, Horton MA (1984) Failure of cells of the mononuclear phagocyte series to resorb bone. Calcif Tissue Int 36:556–558

Clark NB, Fleming WR (1963) The effect of mammalian parathyroid hormone on bone histology and serum calcium levels in *Fundulus kansae*. Gen Comp Endocrinol 3:461–467

Crichton MI (1935) Scale-absorption in salmon and sea trout. Fish Brd Scot Salm Fish 4:1–8

Dhem A (1971) Une cellule géante, l'ostéoclaste. Acta Stomatol Belg 68:213–230

Eastman JT (1977) The pharyngeal bones and teeth of catostomid fishes. Am Midl Nat 97:68–88

Ekanayake S, Hall BK (1987) The development of acellularity of the vertebral bone of the Japanese medaka, *Oryzias latipes* (Teleostei; Cyprinodontidae). J Morphol 193:253–261

Ekanayake S, Hall BK (1988) Ultrastructure of the osteogenesis of acellular vertebral bone in the Japanese medaka, *Oryzias latipes* (Teleostei, Cyprinodontidae). Am J Anat 182:241–249

Francillon H, Meunier FJ, Ngo Tuan Phong D, Ricqlès A de (1975) Données préliminaires sur les structures histologiques du squelette de *Latimeria chalumnae*. II. Tissu osseux et cartilages. In: Lehman JP (ed) Problèmes actuels de Paléontologie: évolution des vertébrés. Colloques Int Cent Natl Rech Scient 287:487–489

Géraudie J, Meunier FJ (1984) Structure and comparative morphology of camptotrichia of lungfish fins. Tissue Cell 16:217–236

Glowacki J, Cox KA, O'Sullivan J, Wilkie D, Deftos LJ (1986) Osteoclasts can be induced in fish having an acellular bony skeleton. Proc Natl Acad Sci USA 83:4104–4107

Hancox NM (1972) The osteoclast. In: Bourne GH (ed) The biochemistry and physiology of bone. Academic Press, New York, pp 45–67

Hirsch JG, Fedorko ME (1968) Ultrastructure of human leukocytes after simultaneous fixation with glutaraldehyde and osmium tetroxide and "postfixation" in uranyl acetate. J Cell Biol 38:615–627

Huysseune A (1986) Late skeletal development at the articulation between upper pharyngeal jaws and neurocranial base in the fish, *Astatotilapia elegans,* with the participation of a chondroid form of bone. Am J Anat 177:119–137

Huysseune A, Verraes W (1986) Chondroid bone on the upper pharyngeal jaws and neurocranial base in the adult fish *Astatotilapia elegans*. Am J Anat 177:527–535

Jones SJ, Boyde A (1977) Some morphological observations on osteoclasts. Cell Tissue Res 185:387–397

Kahn AJ, Stewart CC, Teitelbaum SL (1978) Contact-mediated bone resorption by human monocytes in vitro. Science 199:988–990

Kirschbaum F, Meunier FJ (1981) Experimental regeneration of the caudal skeleton of the glass knifefish, *Eigenmannia virescens* (Rhamphichthydae, Gymnotoidei). J Morphol 168:121–135

Kirschbaum F, Meunier FJ (1988) South American gymnotiform fishes as model animals for regeneration experiments? Monogr Dev Biol 21:112–123

Levi G (1939) Etudes sur le développement des dents chez les Téléostéens. I. Les dents de substitution chez les genres *Ophidium, Trigla, Rhombus, Belone*. Arch Anat Microsc 35:101–146

Lopez E (1970a) Demonstration of several forms of decalcification in bone of the teleost fish, *Anguilla anguilla* L. Calcif Tissue Res 4[Suppl]:83

Lopez E (1970b) L'os cellulaire d'un poisson Téléostéen "*Anguilla anguilla* L.". I. Etude histocytologique et histophysique. Z Zellforsch 109:552–565

Lopez E (1970c) L'os cellulaire d'un poisson Téléostéen "*Anguilla anguilla* L.". II. Action de l'ablation des corpuscules de Stannius. Z Zellforsch 109:566–572

Lopez E, Martelly-Bagot E (1971) L'os cellulaire d'un poisson Téléostéen, *Anguilla anguilla* L. III. Etude histologique et histophysique au cours de la maturation provoquée par injections d'extrait hypophysaire de carpe. Z Zellforsch 117:176–190

Lopez E, Peignoux-Deville J, Lallier F, Martelly E, Millet C (1976) Effects of calcitonin and ultimobranchialectomy (UBX) on calcium and bone metabolism in the eel, *Anguilla anguilla* L. Calcif Tissue Res 20:173–186

Marks SC, Popoff SN (1988) Bone cell biology: the regulation of development, structure, and function in the skeleton. Am J Anat 183:1–44

Meunier FJ (1983) Les tissus osseux des Ostéichthyens. Structure, genèse, croissance et évolution. Thèse de Doctorat d'Etat Paris. Arch Doc Inst Ethnol, micro-édition, Mus Nat Hist Nat, SN 82-600-328, 200 pp

Meunier (1987) Os cellulaire, os acellulaire et tissus dérivés chez les Ostéichthyens: les phénomènes de l'acellularisation et de la perte de minéralisation. Ann Biol 26:201–233

Meunier FJ, Desse G (1978) Interprétation histologique de la "métamorphose radiographique" des vertèbres caudales du saumon (*Salmo salar* L.) lors de sa remontée en eau douce. Bull Fr Pisc 51:33–39

Meunier FJ, Kirschbaum F (1978) Etude anatomique et histologique du squelette axial de *Eigenmannia virescens* (Rhamphichthyidae, Gymnotoidei). Acta Zool (Stockh) 59:215–228

Moss ML (1961) Studies of the acellular bone of teleost fish. I. Morphological and systemic variations. Acta Anat (Basel) 46:343–362

Moss ML (1962) Studies of the acellular bone of teleost fish. II. Response to fracture under normal and acalcemic conditions. Acta Anat (Basel) 48:46–60

Moss ML (1963) The biology of acellular teleost bone. Ann NY Acad Sci 109:337–350

Mundy GR, Altman AJ, Gondek MD, Bandelin JG (1977) Direct resorption of bone by human monocytes. Science 196:1109–1111

Nelson JS (1984) Fishes of the world, 2nd edn. Wiley, New York

Norris WP, Chavin W, Lombard LS (1963) Studies of calcification in a marine teleost. Ann NY Acad Sci 109:312–336

Riehl R (1978) Feinstruktur der Knochenzellen in dem Gonopodium von *Heterandria formosa* Agassiz, 1853 (Teleostei, Poeciliidae). Acta Zool (Stockh) 59:199–202

Riehl R, Holl A, Schulte E (1978) Morphologische und feinstrukturelle Untersuchungen an dem Gonopodium von *Heterandria formosa* Agassiz, 1853 (Pisces, Poeciliidae). Zoomorphologie 91:133–146

Ruben JA, Bennett AF (1981) Intensive exercise, bone structure and blood calcium levels in vertebrates. Nature 291:411–413

Schönbörner AA (1981) Données ultrastructurales et expérimentales sur la résorption des écailles chez les poissons téléostéens. Ichtyophysiol Acta 5:58–62

Sire JY (1985) Fibres d'ancrage et couche limitante externe à la surface des écailles du Cichlidae *Hemichromis bimaculatus* (Téléostéen, Perciforme): données ultrastructurales. Ann Sci Nat Zool 7:163–180

Tchernavin V (1938a) Changes in the salmon skull. Trans Zool Soc (Lond) 24:103–184

Tchernavin V (1938b) The absorption of bones in the skull of salmon during their migration to rivers. Fish Brd Scot Salm Fish 6:1–4

Vaes G (1988) Cellular biology and biochemical mechanism of bone resorption. A review of recent developments on the formation, activation, and mode of action of osteoclasts. Clin Orthop 231:239–271

Van Sommeren VD (1937) A preliminary investigation into the causes of scale absorption in salmon (*Salmo salar* L.). Fish Brd Scot Salm Fish 11:1–11

Weiss RE, Watabe N (1979) Studies on the biology of fish bone. III. Ultrastructure of osteogenesis and resorption in osteocytic (cellular) and anosteocytic (acellular) bones. Calcif Tissue Int 28:43–56

Wendelaar Bonga SE, Lammers PI (1982) Effects of calcitonin on ultrastructure and mineral content of bone and scales of the cichlid teleost *Sarotherodon mossambicus*. Gen Comp Endocrinol 48:60–70